LASER-BASED POSE-TRACKING OF A WHEELED MOBILE ROBOT

Ching-Chih Tsai, Hung-Hsing Lin, Kim-Hon Wong

Department of Electrical Engineering, National Chung-Hsing University
Taichung, Taiwan, R.O.C

Abstract: This paper develops methodology and technique for pose tracking of an autonomous mobile robot (AMR) using a laser scanner. A low-complexity and accurate pose-tracking EKF-based algorithm is proposed using a simple rectangular model and a 2-D laser scanner. By continuously updating the robot's pose and matching the laser data with the environmental model, we find that the outliers can be filtered out effectively by validation gate. Moreover, a Range-Weighted Hough Transform (RWHT) is used to extract the modeled lines from the clutter data. Numerous simulations and experimental results are provided to verify the feasibility and effectiveness of the proposed pose-tracking method.

Keywords: pose-tracking, laser scanner, mobile robot, navigation, Range-Weighted Hough Transform.

1. INTRODUCTION

This paper is concerned with the problem of developing methodologies and techniques for pose-tracking of an autonomous mobile robot (AMR) using a 2-D laser scanner. AMR, a kind of free-ranging guided vehicle, has already found successful applications in structured environments such as automatic factories, offices, and hospitals. It has also been utilized to perform some special missions in unstructured dangerous or complex environments for relieving dangerous risks of natural disasters, battlefields, and so on.

The pose-tracking ability is necessary for reactive, planned, or hybrid navigation of the AMR. Generally speaking, the localization problem can be divided into three subproblems: pose-tracking, pose initialization, and map acquisition. When the AMR is moving in the environment and the initial pose of the robot is known, the process of keeping track of the pose of the robot is referred to as pose-tracking. Pose-tracking can be used if the initial estimate of the pose is given. However, in some situations, the initial pose of AMR is unknown. Therefore, the process of finding the starting pose of the robot with no prior pose information is called pose initialization or global localization. In addition, the map acquisition problem is referred as the simultaneously localization and map building (SLAM), where a robot starts in an unknown location in an unknown environment and then incrementally builds a map present in this environment while simultaneously using this map to compute the pose of robot. However, this paper only focuses on addressing the pose-tracking problems.

The dead-reckoning method based on the encoded or odometric information from the driving wheels has been extensively utilized to calculate the current pose of the AMR. However, this method suffers from the accumulation errors by wheel slippage, or by mechanical tolerances and surface roughness. Hence, the robot may fail to keep track of its true pose over long distances. To overcome the shortcoming, some external sensors, such as laser, ultrasonics and visual sensors, have been adopted and incorporated with the sensor fusion techniques to improve the accuracy and reliability of the localization system. Hence, this paper develops a novel pose-tracking system and method using the laser scanner measurements.

The laser scanner system has been considered as a powerful and accurate alternative for self-localization of the robot. For mobile robot navigation, laser sensors can be divided into two technical methodologies: one is the angle-measuring laser scanner with artificial reflector landmarks detection; the other is the most popular range-measuring time-of-flight (TOF) laser. Only a few studies have been focused on the angle-measuring laser scanner Decker *et al.*(1992) and Chang *et al.*(2003), but plenty of studies have been done regarding to the applications of a laser range finder to localization problem (Jensfelt and Christensen (1999); Forsberg *et al.*(1993)). In the pose-tracking problem, the type of laser range finder has been studied by Forsberg *et*

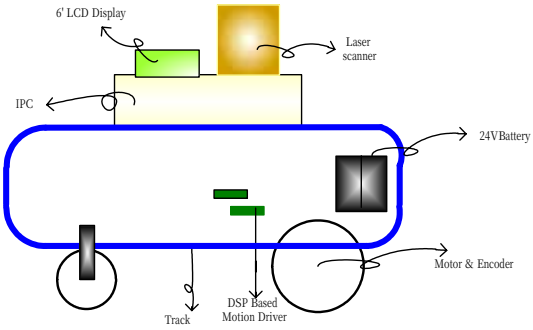

Fig. 1 Physical configuration of the autonomous mobile robot

Fig. 2 A photograph of the proposed mobile robot system

al.(1995). Kim (1993) proposed a hierarchical navigation system and the use of laser range finder for the localization of a mobile robot. Jensfelt *et al.* (2001) presented a Kalman filter-based approach utilizing 2-D laser scanner for pose-tracking of a mobile robot. In this paper, we will propose an extended Kalman filter approach utilizing a rectangular environmental model for pose-tracking of an AMR.

The remaining parts of this paper are organized as follows. A complete description of the proposed autonomous mobile robot system is presented in Section 2. Section 3 presents the pose-tracking algorithm based on the EKF approach. Section 4 shows the experimental results for the pose-tracking approach. Section 5 states the conclusions.

2. DESCRIPTION OF THE AUTONOMOUS MOBILE ROBOT AND CONTROL SYSTEM

Fig.1 shows the control architecture of the autonomous mobile robot and control system whose mobile platform is based on the basic structure of a wheeled vehicle system. There are two motors mounted on the right and left wheels, thereby giving rise to differential driving motion. The robot can move on both even and uneven terrains. The length of the robot is 90cm, the width 70cm, the height 40cm, and the weight 55 kgw.

Fig. 2 depicts a photograph of the experimental mobile robot. The robot comprises four parts : a

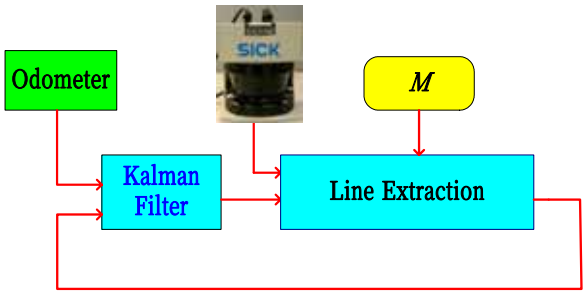

Fig. 3 Block diagram of the feature-based pose-tracking algorithm

power management module, an IPC-based computational unit, the motion control system and the laser scanning system. The main function of the motion control system is to provide precise velocity control for the two DC 24V motors. The main closed-loop control laws of the two DC motors with encoders are the conventional PI (Proportion-Integration) control laws implemented by two low-cost single-chip digital signal processors, DSP TMS320C240, from Texas Instrument Co. Two optical encoders mounted on the motor shafts are used to obtain the speed and traveling distance of the vehicle. Two quadrature pulses, ϕ_A and ϕ_B, are further processed by a PIC-based counter and then sent out the motor's velocities and rotation directions to the industrial IPC via an 8255 digital interfacing card. The industrial PC uses the dead-reckoning method to find the current position and orientation of the robot.

The vehicle driver system requires a DC 24V power, offered by two serial DC 12V batteries, delivering sufficient power to drive the two motors. The 24V power supply outputs a maximum DC current up to 10 Amps. This computation unit with a CPU speed of 800MHZ is powered by a power supply of DC 24V. The power supply for the IPC comes from an extra power source, in order to make the vehicle light and easy to move.

The Laser Measurement System (LMS) is a non-contact measuring system, which scans its two-dimensional surroundings. The LMS is based on a time-of-flight measurement principle. A single laser pulse is emitted and reflected by an object surface within the range of the sensor. The elapsed time between emission and reception of the laser pulse serves to calculate the distance between any object and the LMS. The laser scanner does not need any reflectors to function as a scanning system. The laser pulses sweep a radial range in front of the LMS platform via an integrated rotating mirror.

3. POSE-TRACKING ALGORITHM

This section describes how to construct a pose-tracking algorithm using the well-known extended Kalman filter (EKF); especially, special efforts will be paid to study how the measurement

model is established and how the wall features are represented and extracted. For tracking the pose of the robot, we have two measurements from the odometer and the laser scanner. The odometer can be used for pose-tracking of the robot over short traveled distances, and the laser scanner is adopted to attain distance information between the vehicle and its surrounding; these two measurements together with the environmental model will be used to find the absolute pose of the mobile robot. Fig. 3 displays a block diagram of the proposed feature-based pose-tracking algorithm.

3.1 Environmental Model

In order to develop a low-complexity pose-tracking system, we here use a simple rectangular model as the environmental model. The rectangular model is a simple case of a line-based model. The main advantage of using the rectangular model is very likely to develop a robust pose-tracking method. Fig. 3 depicts the model, where M denotes the environmental model composed of a set of walls, m_i, i.e.

$$M = \{m_i, i = 1,...., N\}$$

where m_i is denoted by $(\rho_i^m, \alpha_i^m, l_i^m)$, ρ_i^m is the distance to the ith modeled wall with respect to the world frame, α_i^m is the corresponding angle, l_i^m is the length of the wall. Fig.4 shows the parameters defined for the environmental model, where superscript (W) and (R) represent the world coordinate system and robot coordinate system respectively.

3.2 Measurement Model

A line segment can in principle constrain all three degrees of freedom of a mobile robot. To describe the walls associated with the rectangular model extracted from laser range data, we use the 3-tuple (ρ, α, l), where ρ is the perpendicular distance from robot to the line, α is the orientation of the line, and l is the length of the line. The length of the line is employed to reduce the risk of making errors in data association. Fig. 4 shows the parameters definition of a wall.

For the pose estimate in an extended Kalman filter framework, we need to predict the parameters of the walls to be extracted from the current state of the robot and the environmental model. Therefore two parameters ρ and α are considered to be measurements in the EKF framework. A wall measurement equation can be modeled as

$$z(k) = h(x(k)) + v(k) \quad (1)$$

or,

$$\hat{z}_i = \begin{bmatrix} \hat{\rho}_i \\ \hat{\alpha}_i \end{bmatrix} = h_i(X, M) + v_i \quad , \quad i = 1, 2, ..., N \quad (2)$$

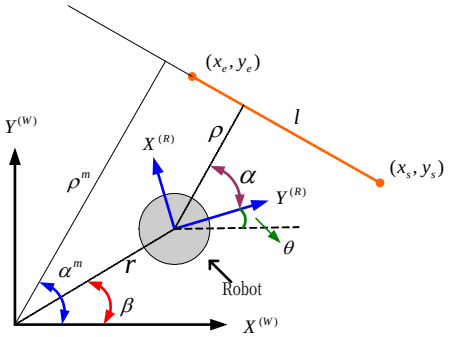

Fig. 4 The parameters defining a wall

where v_i is the measurement noise, M denote the model of the walls and subscript i represents the ith walls. The measurement function $h_i(X, M)$ can be expressed by

$$h_i(X, M) = \begin{bmatrix} \rho_i^m - \sqrt{x^2 + y^2}\cos(\alpha_i^m - \beta) \\ \alpha_i^m - \theta \end{bmatrix} \quad (3)$$

where ρ_i^m is the distance to the ith modeled wall with respect to the world coordinate system and α_i^m is the corresponding angle. Fig. 4 shows an illustration of the parameters defining a wall, where (x_e, y_e) and (x_s, y_s) are the starting and end point of the wall, l is the length of the wall, r is the distance between the current poses of the robot and the origin of the world coordinate system, and β is the corresponding angle.

The measurement function can be expressed as the following linear term:

$$z_i = H_i X + m_i \quad (4)$$

where the Jacobian matrix H_i with respect to the state X is given by

$$H_i = \left.\frac{\partial h}{\partial X}\right|_{X = \hat{X}(k/k-1)} = \begin{bmatrix} H_{11} & H_{12} & 0 \\ 0 & 0 & -1 \end{bmatrix} \quad (5)$$

where the elements of H_i are given by

$$H_{11} = -\frac{x}{r}\cos(\alpha_i^m - \beta) - \frac{y}{r}\sin(\alpha_i^m - \beta) \quad (6)$$

$$H_{12} = -\frac{y}{r}\cos(\alpha_i^m - \beta) + \frac{x}{r}\sin(\alpha_i^m - \beta) \quad (7)$$

Note that $r = \sqrt{x^2 + y^2}$, $\beta = \arctan\left(\frac{y}{x}\right)$

3.3 EKF-Based Pose-Tracking Algorithm

As the mobile robot moves in the rectangular model, the initial pose of the robot is assumed to be known. By using the priori pose information and the environmental model, an EKF-based pose-tracking algorithm is proposed to update the robot pose estimate. The state equation describing the kinematics of the mobile robot can be expressed by

$$X(k+1) = f(X(k)) + W(k) \quad (8)$$

$$\text{or,}\quad \begin{bmatrix} x_c(k+1) \\ y_c(k+1) \\ \theta(k+1) \end{bmatrix} = \begin{bmatrix} x_c(k) + \Delta d \cos\theta(k) \\ y_c(k) + \Delta d \sin\theta(k) \\ \theta(k) + \Delta\theta \end{bmatrix} + \begin{bmatrix} w_x(k) \\ w_y(k) \\ w_\theta(k) \end{bmatrix} \quad (9)$$

where $\Delta\theta = \Delta T \cdot w_c$, $\Delta d = \Delta T \cdot v_c$, ΔT is the sampling interval, v_c and w_c is the linear and angular velocities of the robot, respectively. The process noises $w_x(k)$, $w_y(k)$ and $w_\theta(k)$ denote the uncertainties due to the wheel slippage, surface roughness, etc.; they are modeled as uncorrelated zero-mean white Gaussian processes with covariance matrix $Q(k) = diag\{\sigma_{wx}^2, \sigma_{wy}^2, \sigma_{w\theta}^2\}$. In order to obtain the best pose estimate of the mobile robot, a discrete-time extended Kalman filter algorithm is briefly proposed as follows:

Step1: At the time $k = 0$, select a good estimate $\hat{X}(0/0)$ and an initial error covariance matrix $\tilde{P}(0/0)$, where

$$E\{X(0/0)\} = \hat{X}(0/0)$$

$$E\left\{\left|X(0) - \hat{X}(0)\right| \cdot \left|X(0) - \hat{X}(0)\right|^T\right\} = \tilde{P}(0/0)$$

Step2: Let the optimal estimate of $X(k)$ at time k be $\hat{X}(k/k)$ and its error covariance matrix be $\tilde{P}(k/k)$. Use Eqs. (10) and (11) to calculate the best prediction, $X(k+1/k)$ and its propagation error covariance $\tilde{P}(k+1/k)$.

$$\hat{X}(k+1/k) = f(\hat{X}(k/k)) \quad (10)$$

$$\tilde{P}(k+1/k) = F(\hat{X}(k/k)) \cdot \tilde{P}(k/k) \cdot F(\hat{X}(k/k))^T + Q(k) \quad (11)$$

where

$$F(\hat{X}(k/k)) = \frac{\partial f(X(k))}{\partial X(k)}\bigg|_{\hat{X}(k/k)} = \begin{bmatrix} 1 & 0 & -\Delta d \sin\theta \\ 0 & 1 & \Delta d \cos\theta \\ 0 & 0 & 1 \end{bmatrix} \quad (12)$$

Step3: At time $k+1$, the location system reads the measurement data $Z(k+1)$ and then uses Eqs. (13) and (14) to obtain the updating estimate $\hat{X}(k+1/k+1)$ and the error covariance matrix $\tilde{P}(k+1/k+1)$.

$$\hat{X}(k+1/k+1) = \hat{X}(k+1/k) + K(k+1) \cdot \left[Z(k+1) - h\left(\hat{X}(k+1/k), M\right)\right] \quad (13)$$

$$\tilde{P}(k+1/k+1) = \left[I - K(k+1)_i \cdot H_i\right] \cdot \tilde{P}(k+1/k) \quad (14)$$

$$K(k+1) = \tilde{P}(k+1/k) \cdot H_i^T \left[H_i \cdot \tilde{P}(k+1/k) \cdot H_i^T + R(k+1)\right]^{-1} \quad (15)$$

where

$$H_i = \frac{\partial h}{\partial X}\bigg|_{X=\hat{X}(k/k-1)} = \begin{bmatrix} H_{11} & H_{12} & 0 \\ 0 & 0 & -1 \end{bmatrix} \quad (16)$$

Step 4: Repeat ***Step 2*** to ***Step 3***.

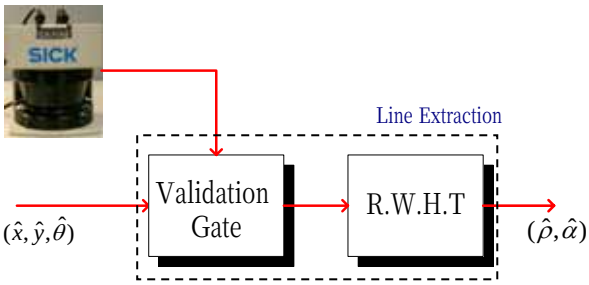

Fig. 5 Block diagram of line extraction algorithm

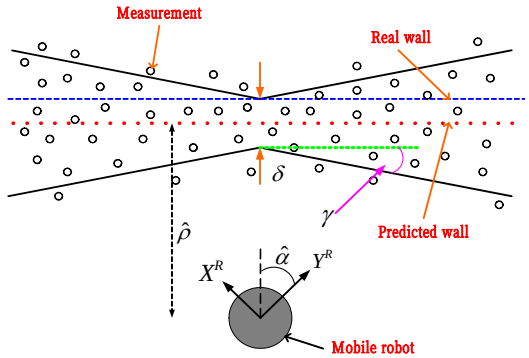

Fig. 6 Validation gate

3.4 Line Extraction

In a rectangular room, the walls constitute the features that we want to track. Lines are used to describe the walls because the description of a line is very simple. By using three well-defined parameters: ρ, the perpendicular distance from robot to the line, α, the orientation of the normal, l, the length, which are the parameter vector of a line. We express a line equation with the two parameters ρ and α as

$$\rho = x\cos\alpha + y\sin\alpha \quad (17)$$

Assuming that the estimate of the robot pose is known, the pose of a modeled wall can be predicted. We propose a one-step approach to extract a wall model from the cluttered laser data. The design goal is twofold: 1) classify each data point as belonging to a particular model wall or as an outlier and 2) estimate the parameters of the model walls. For this task, we propose to use a line extraction algorithm. The algorithm includes a range-weighted Hough transform together with a validation gate. Fig. 5 depicts the block diagram of the line extraction algorithm according to the feature-based pose-tracking.

3.4.1 Validation Gate

In the target tracking literature, the issue of data association has always been in focus. The use of validation gates is a common method to manage such a problem. A validation gate defines a region around some predicted value in which a measurement will be accepted as associated with the corresponding feature. The purpose of using validation gate is to filter out data points that are likely to be associated with the corresponding walls. Then, we can extract the parametric description of these walls in the form of

lines. Due to the clutter, the walls might be difficult to extract without prefiltering.

We define the location of the gates be functions of the estimated robot pose and the local room model. The size of the gates will depend on the quality of the laser data and the uncertainty in the environmental model. If the uncertainty in the pose grows or the laser data is very noisy, the gates will be opened up and let more data through the gates. Let the validation gate region be described by the four-tuple

$$G = (\hat{\rho}, \hat{\alpha}, \delta, \gamma)$$

where $\hat{\rho}$ and $\hat{\alpha}$ define the pose of the gate, δ and γ define the size of the gate. The illustration of the parameters that define the size and location of the validation gate is shown in Fig. 6. We observe in Fig. 6 that $\hat{\rho}$ is the predicted distance to the wall and $\hat{\alpha}$ is the predicted angle of the normal to the wall, δ is the smallest width of the gate and γ is the opening angle.

3.4.2 Range-Weighted Hough Transform

The Hough Transform (HT), due to Hough (1959), is one of the most often used algorithms in image analysis and computer vision. The algorithm is known as a popular and powerful technique for detecting and estimating the parameters of multiple lines that are present in a noisy range measurement.
In this paper, a modified Hough transform is used, which is called Range-Weighted Hough Transform (RWHT). This version of RWHT is aimed at extracting the orientations, α, and distances ρ to the walls of the environmental model. The RWHT is a robust parameter estimator, but it is computationally expensive. It could still be sensitive to spurious range measurements.

The basic idea of this technique is to transform between the Cartesian space (r, ϕ) and a parameter space (ρ, α) in which a wall can be defined. The RWHT $C(\rho, \alpha)$ can be defined as the following function:

$$C(\rho, \alpha) = \sum_i w\ (\ r_i \cos(\phi_i - \alpha) - \rho\ )\ r_i \qquad (18)$$

where $w(x)$ be a unit rectangular window function of width a. Moreover, $w(x)$ can be defined as

$$w(x) = \begin{cases} 1 & , \ |x| \le a \\ \\ 0 & , \ |x| > a \end{cases} \qquad (19)$$

The argument in w is equal to the shortest distance between the range measurements (r_i, ϕ_i) and the wall (ρ, α). The parameters are described in Fig. 7. As shown in Fig. 8, the RWHT $C(\rho_i, \alpha_i)$ is defined as the number of measurements inside the strip with width a centered around the wall (ρ, α). This algorithm computes an accumulator array that holds

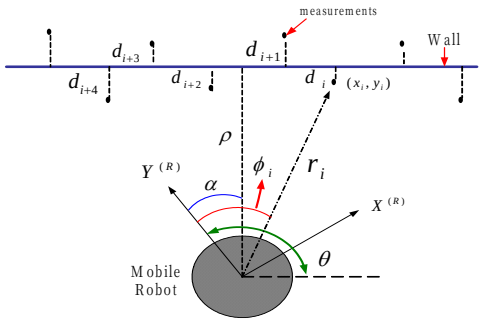

Fig. 7 Observations (r_i, ϕ_i) with robot orientation θ

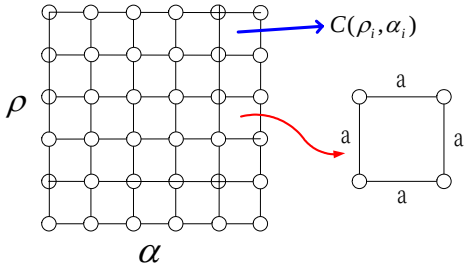

Fig. 8 Parameter space

the evidence for a feature for each set of parameters. The RWHT proceeds with each range measurement in Cartesian space being transformed to a region in parameter space. When the region intersects one of the strips, the corresponding accumulator is increased. Moreover, the RWHT $C(\rho, \alpha)$ can be transformed into a histogram. The highest peak in the RWHT histogram means that its accumulator has the most votes. Each peak in the histogram gives an estimate of the distance ρ and the corresponding orientation α of the wall. To extract the walls reliably, the method for obtaining the parameters (ρ, α) of the wall is performed as follows:

Step 1: Search the single highest peak in the RWHT histogram.

Step 2: Remove the measurements associated with this peak from the RWHT.

Step 3: Repeat ***Step 1*** until all major peaks have been found.

4. EXPERIMENTAL RESULTS AND DISCUSSION

This section is devoted to conducting two experiments for showing the feasibility and efficiency of the proposed pose-tracking scheme. To do so, let the mobile robot move in a straight-line manner within the environment model. The total distance traveled in each experiment was 200cm; the constant linear velocity was $v_c = 1\, cm/s$. These experiments were conducted in the rectangular model which is approximately 236cm× 420cm with respect to the world model. The four parameters of environment model are $(\rho_1^m, \alpha_1^m) = (20.86, -10^\circ)$, $(\rho_2^m, \alpha_2^m) = (54.45, 80^\circ)$, $(\rho_3^m, \alpha_3^m) = (256.86, -10^\circ)$, $(\rho_4^m, \alpha_4^m) = (474.45, 80^\circ)$. Assume that the initial

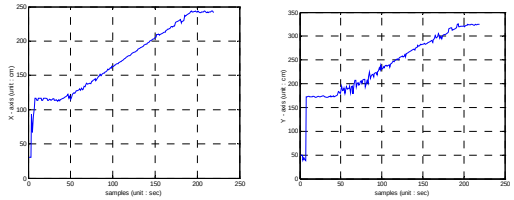

Fig. 9(a) Time history of the robot pose estimates

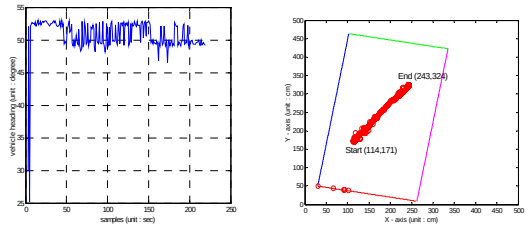

(b) (c)

Fig. 9(b) Robot heading estimates
(c) The x-y robot trajectory

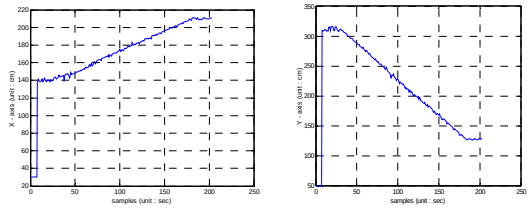

Fig. 10(a) Time history of the robot pose estimates

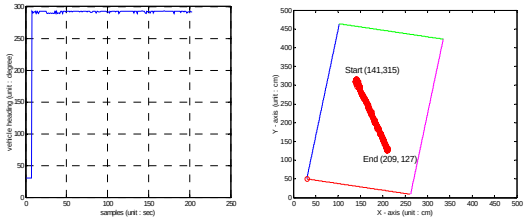

(b) (c)

Fig. 10(b) Robot heading estimates
(c) The x-y robot trajectory

estimate was $\hat{X}(0/0) = [30,\ 50,\ 30^\circ]^T$; the size of the validation gate, $\delta = 2\ cm$, $\gamma = 2^\circ$; the distance and angle resolution of RWHT are $2.5\,cm$ and 2.5°. The matrices $R = diag\{0.0000025, 0.0000025\}$ and $Q = diag\{0.001, 0.001, 0.001\}$ were considered for initializing the error covariance matrices.

Experiment 1: The robot started at the position (114,171) with the vehicle heading angle of 50 degrees and stopped at the position (243,324) with respect to the world model. The x-y trajectory of the robot's pose estimate is shown in Fig. 9(a). Fig. 9(b) depicts the heading estimates. Fig. 9(c) displays the actual measurements of the robot with respect to the world model.

Experiment 2: The robot started at the position (141,315) with a vehicle heading of 290 degrees and stopped at the position (209,127) with respect to the world model. Fig. 10(a) presents the time history of the robot's pose estimate, and Fig. 10(b) depicts the heading estimates. Fig.10(c) displays the actual measurements of the robot with respect to the world model.

Through the experimental results, the proposed pose-tracking algorithm has been proven capable of giving a satisfactory performance to continuously track the robot posture in the environment.

5. CONCLUSIONS

This paper has presented a robust, low-complexity, and accurate pose-tracking algorithm based on a rectangular model and a 2-D LMS. The rectangular model provides robustness using only the large-scale features. Such features are very simple and robust. With the EKF algorithm, the pose-tracking scheme fuses the measurements from odometer and laser scanner to obtain the optimal orientation and location estimate of the robot corresponding to the world frame. Several experimental results have shown that the proposed pose-tracking scheme performs well in the situations under consideration.

ACKNOLEDGEMENT

The authors gratefully acknowledge financial support from the National Science Council, Taiwan, the Republic of China, under grant NSC92-2213-E-005 -009

REFERENCES

Decker, S., Gander, H., Vincze, M., and Prenninger, J. P., Dynamic Measurement of Position and Orientation of Robots, *IEEE Trans. Instrumentation and Measurement*, vol. 41, no. 6, pp. 897-901, December 1992.

Chang, C. F., Tsai, C. C., Hsu, J. C., Lin, S. C., and Lin, C. C., Laser-Based Beacon Localization for an Autonomous Mobile Robot, Submitted to the 2003 *IEEE International Conference on Automation, Technology*, Taipei, Taiwan, R.O.C.

Jensfelt, P., and Christensen, H. I., Laser Based Pose Tracking, Proceeding of the 1999 *IEEE International Conference on Robotics & Automation*, vol. 4, pp. 2994-3000, May 1999.

Forsberg, J., Larsson, U., Ahman, P., and Wernersson, A., The Hough Transform inside the Feedback Loop of a Mobile Robot, Proceeding of the *IEEE International Conference on Robotics & Automation*, vol. 1, pp. 791-798, May 1993.

Forsberg, J., Larsson, U., and Wernersson, A., Mobile Robot Navigation using the Range-Weighted Hough Transform, *IEEE Robotics & Automation Magazine*, vol. 2, pp. 18-26, March 1995.

Kim, Y. H., Localization of a Mobile Robot using a Laser Range Finder in a Hierarchical Navigation System, *IEEE Proc. of Southeastcon* '93, 1993.

Jensfelt, P., and Christensen, H. I., Pose Tracking using Laser Scanning and Minimalistic Environmental Models, *IEEE Transactions on Robotics and Automation*, vol. 17, no. 2, April 2001.